Plastic strain localization in surface-hardened titanium polycrystals

E S Emelianova[1, 2] and V A Romanova[2]

[1]National Research Tomsk State University, Faculty of Physics and Engineering, 634050 Tomsk, Russia
[2]Institute of Strength Physics and Materials Science SB RAS, Laboratory of Mechanics of Heterogeneous Materials, 634055 Tomsk, Russia

E-mail: emelianova@ispms.ru

Abstract. In this paper, features of plastic strain localization in commercial purity titanium surface-hardened by ultrasonic impact treatment (UIT) are numerically investigated. Three-dimensional polycrystalline structures inherent in unhardened and UIT surface-hardened titanium specimens are generated by a step-by-step packing method. For taking into account the deformation mechanisms at the micro- and mesoscales, constitutive equations describing a nonlinear behavior of individual grains are constructed using crystal plasticity theory. Quasi-static boundary value problems are solved in a dynamic statement using ABAQUS\Explicit finite-element package to simulate uniaxial tension of the model polycrystalline specimens. Based on the calculation results, conclusions are drawn on the effect of the UIT surface-hardened layer on the plastic strain localization and deformation-induced surface roughening in model polycrystals.

1. Introduction

Titanium alloys are widely used in aircraft, shipbuilding, medical equipment manufacturing and other industrial applications. To improve the strength characteristics of titanium alloys, various surface treatment methods are used, one of which is ultrasonic impact treatment (UIT). This method results in the grain refinement and appearance of a basal texture in a subsurface layer [1-6]. The UIT-modified subsurface layer prevents early appearance of plastic strain on the surface and its propagation in the bulk. At the same time, due to a significant difference in the grain size on the surface and in the bulk of the material, additional stress concentration and plastic strain localization can appear near the grain boundaries.

Although the thickness of a surface-hardened layer is about 100-200 μm, the experimental data show a significant increase in the strength properties of the UIT surface-hardened materials [1-4]. Commonly used macroscopic models where the material constituents contribute to the overall material response proportionally to their volume fraction fail to describe this phenomenon. In this paper the influence of the UIT surface-hardened layer on the deformation behavior of commercial purity titanium is investigated numerically in terms of micromechanics. The effect of the microstructure and texture on plastic strain localization on the surface and in the bulk of model polycrystals is discussed.

Content from this work may be used under the terms of the Creative Commons Attribution 3.0 licence. Any further distribution of this work must maintain attribution to the author(s) and the title of the work, journal citation and DOI.
Published under licence by IOP Publishing Ltd

2. Microstructure-based model

The electron backscatter diffraction (EBSD) analysis has shown that the microstructure of unhardened commercially pure titanium is characterized by randomly oriented equiaxed grains with an average size of about 70 μm (figure 1a). The UIT gives rise to the formation of a basal texture in a subsurface layer where the grain size decreases up to 20 μm (figure 1b) [1-6].

Based on the experimental data [1, 4], two model three-dimensional microstructures (figure 2) were generated by the step-by-step packing method [7]. The first microstructure (figure 2a) contains 2808 equiaxed grains with an average grain size of 70 μm and has no texture (figure 3a), which corresponds to an unhardened specimen. The second microstructure (figure 2b) contains 6000 equiaxed grains, of which 5000 grains belonging to the subsurface layer are characterized by an average grain size of 20 μm and a basal texture (figure 3b). This corresponds to the UIT surface-hardened material. Both model microstructures were generated on regular 900×300×900 μm meshes containing $11 \cdot 10^6$ hexahedral elements.

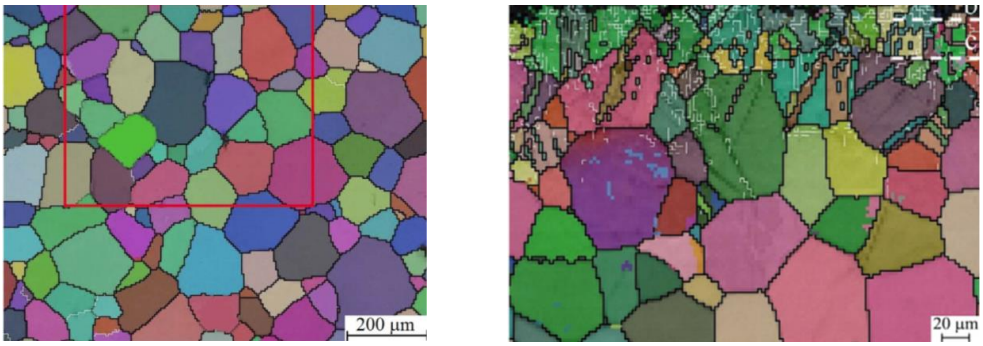

(a) (b)

Figure 1. EBSD maps of the as-received (a) and UIT-modified titanium specimens (b) [1, 4].

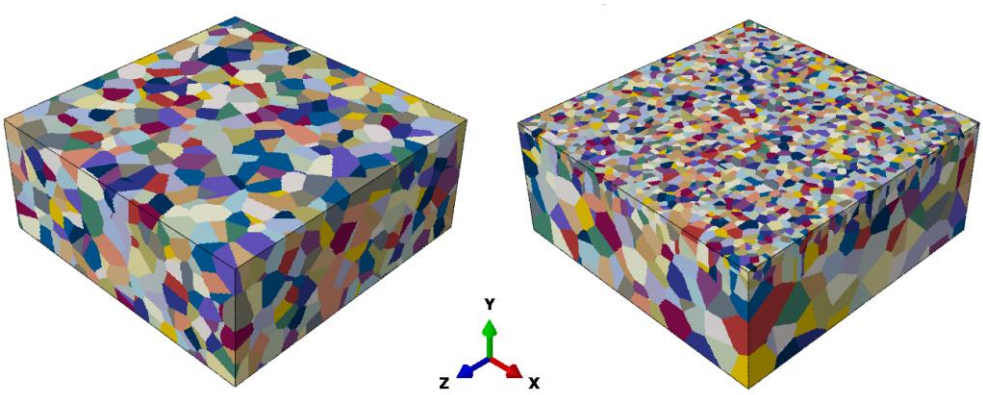

(a) (b)

Figure 2. Model microstructures of unhardened (a) and UIT surface-hardened materials (b).

Crystallographic orientations of grains were defined by a set of Bunge Euler angles $\varphi_1 \Phi \varphi_2$. The absence of texture was described by randomly generating Euler angles, while the basal texture was set by Euler angles varying in the range $175^\circ \le \varphi_1 \le 185^\circ$, $85^\circ \le \Phi \le 95^\circ$, $0^\circ \le \varphi_2 \le 360^\circ$. Direct (0001) and $(10\bar{1}0)$ pole figures for the subsurface grains of the unhardened and surface-hardened polycrystals are shown in figure 3.

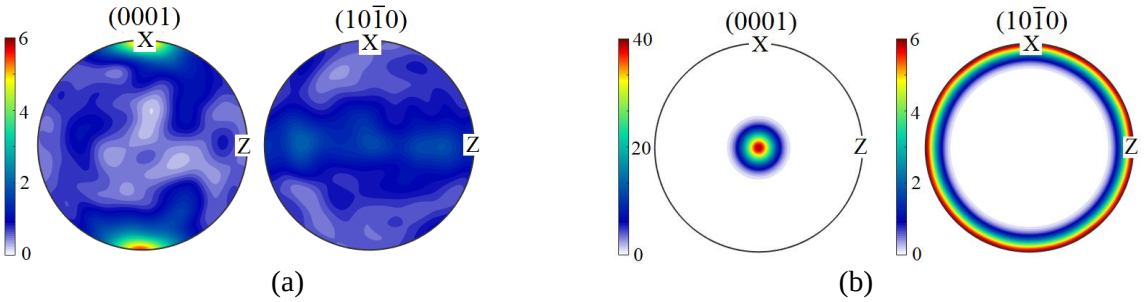

Figure 3. (0001) and $(10\bar{1}0)$ pole figures for subsurface layers of polycrystalline titanium models.

Constitutive equations describing the deformation behavior of individual grains (single crystals) are written in terms of anisotropic elasticity and crystal plasticity theories. To describe the anisotropic elastic behavior, the generalized Hooke's law is used, written down taking into account the representation of the total strain tensor ε_{ij} as the sum of the elastic ε_{ij}^{e} and plastic ε_{ij}^{p} components:

$$\dot{\sigma}_{ij} = C_{ijkl}\left(\dot{\varepsilon}_{kl} - \dot{\varepsilon}_{kl}^{p}\right). \tag{1}$$

Here σ_{ij} are the stress tensor components, C_{ijkl} is the tensor of elastic moduli. The dot above the symbol indicates the time derivative.

The plastic strain tensor is defined in the framework of the crystal plasticity approach. It explicitly takes into account features of dislocation glide on active slip systems in metals with a hexagonal close-packed lattice:

$$\dot{\varepsilon}_{ij}^{p} = \sum_{\alpha} \dot{\gamma}^{(\alpha)} \frac{1}{2}\left(s_i^{(\alpha)} m_j^{(\alpha)} + s_j^{(\alpha)} m_i^{(\alpha)}\right). \tag{2}$$

Here $s_i^{(\alpha)}$ and $m_j^{(\alpha)}$ are the slip direction and slip plane normal vectors, respectively. The shear strain rate $\dot{\gamma}^{(\alpha)}$ on the slip system α is defined as a function of the resolved shear stress $\tau^{(\alpha)} = s_i^{(\alpha)} \sigma_{ij} m_j^{(\alpha)}$ following the power law [8]:

$$\dot{\gamma}^{(\alpha)} = \dot{\gamma}_0 \left| \frac{\tau^{(\alpha)}}{\tau_*^{(\alpha)}} \right|^{\nu} sign\left(\tau^{(\alpha)}\right). \tag{3}$$

Here $\dot{\gamma}_0$ is the reference shear strain rate, ν is the strain rate sensitivity coefficient, $\tau_*^{(\alpha)}$ is the critical resolved shear stress (CRSS) activating the slip system α:

$$\tau_*^{(\alpha)} = \tau_0^{(\alpha)} + k_1 D^{-1/2} + k_2 \varepsilon_{eq}^{p}. \tag{4}$$

Here ε_{eq}^{p} is the accumulated equivalent plastic strain, $\tau_0^{(\alpha)}$ is the initial CRSS activating the α slip system in a single crystal; k_1, k_2 are the fitting coefficients, and D is the grain diameter calculated as a diameter of a sphere of the same volume.

The model microstructures undergo uniaxial tension along the X-axis, the other surfaces are taken to be symmetry planes or free of forces. Constitutive microstructure-based models are imported in ABAQUS/Explicit through VUMAT User Subroutine. Note that we solve the quasi-static problem in terms of dynamics which allows efficient calculating for large meshes [9-11].The mathematical formulation of the boundary value problem is given in more detail in [4].

3. Results and discussion

Three-dimensional finite-element calculations of uniaxial tension along X-axis were performed for the unhardened and UIT surface-hardened titanium specimens. Figures 4 and 5 show the calculated

equivalent stress (figure 4) and plastic strain (figure 5) patterns for different degrees of strains. From the onset of plastic deformation, these patterns demonstrate a strong inhomogeneity at the grain scale due to a limited set of slip systems that can be activated at the room temperature under quasi-static loading. As a result, individual grains unfavorably oriented with respect to the loading axis are deformed elastically or involved in plastic deformation in a later stage of loading. The strain accommodation of these grains occurs due to their rigid rotation or plastic strain and rotation of neighboring grains.

A higher level of stresses is observed in the subsurface layer of the UIT surface-hardened material. This is due to a reduced grain size, which is taken into account through the Hall–Petch relation (the second term in the right-hand side of equation (4)). The stress concentration and plastic strain localization occur near the grain boundaries. The smaller the grain size is, the more the localization areas appear.

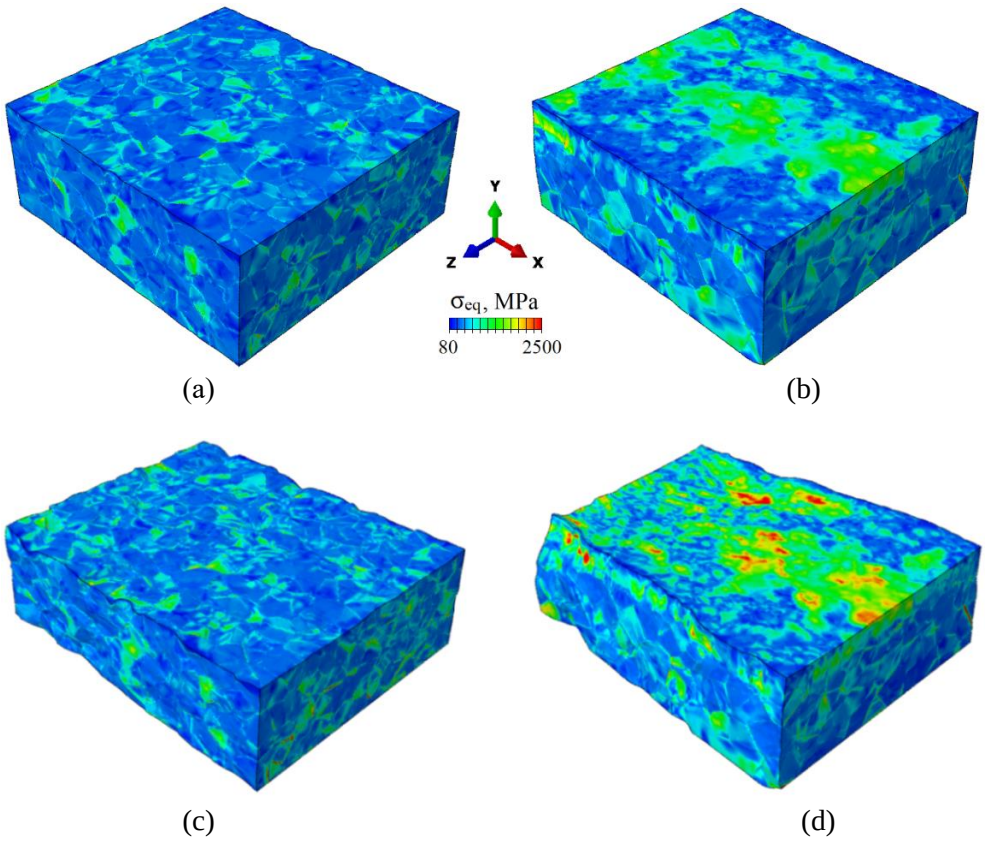

Figure 4. Calculated equivalent stress fields in the unhardened (a, c) and UIT surface-hardened polycrystals (b, d) at 5% (a, b) and 20% tensile strains (c, d).

Generally, a grain can simultaneously experience rotation and dislocation slip [3]. The experimental evidence of this behavior is discussed in [4]. In terms of mechanics, the rigid rotation of a grain does not contribute to the stress-strain state. Plastically undeformed grains exhibit a higher level of stress.

At the mesoscale, plastic deformation is characterized by multiple noncrystallographic shear bands passing through entire groups of grains regardless of their orientations and covering the entire surface of the specimen. In the UIT surface-hardened polycrystal, the mesoscale shear bands seen on the free surface lie at an angle of 45 degrees to the loading axis and are perpendicular to the loading axis on the lateral sides. Contrastingly, in the unhardened polycrystal, the mesobands are perpendicular to the loading axis on the free surface and directed at an angle of 45 degrees at the lateral sides. This

behavior is in a good agreement with experimental data, which additionally validates the numerical model.

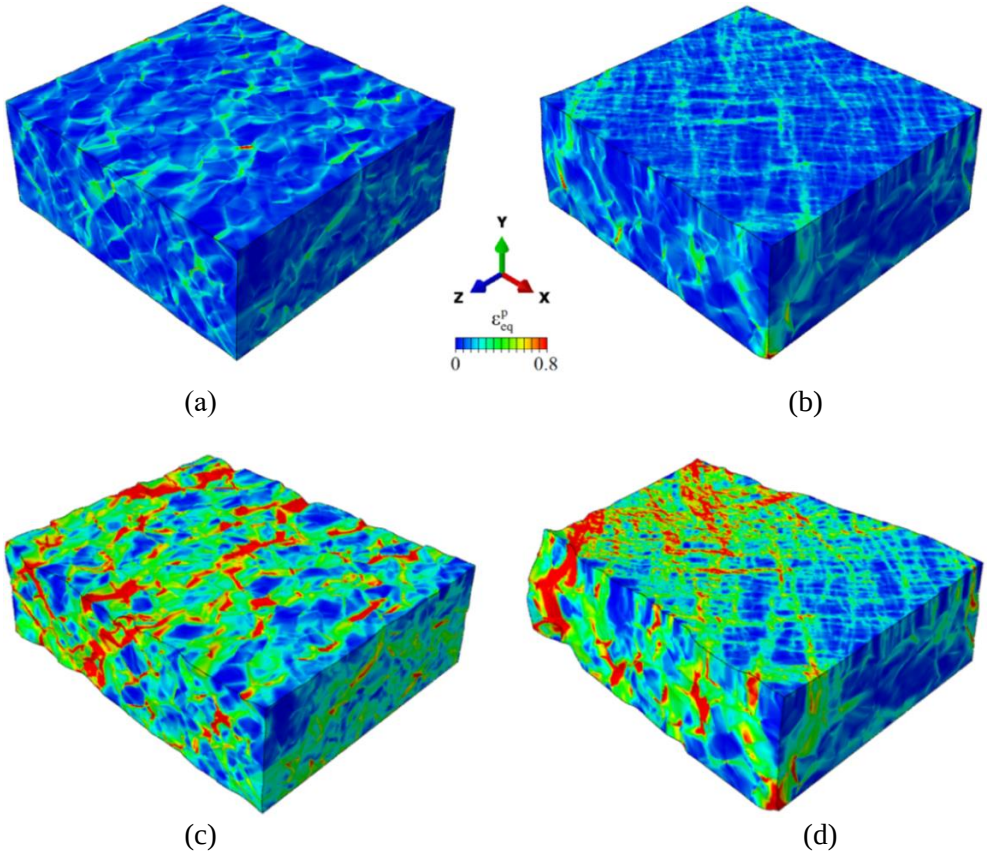

Figure 5. Calculated plastic strain fields in the unhardened (a, c) and UIT surface-hardened polycrystals (b, d) at 5% (a, b) and 20% tensile strains (c, d).

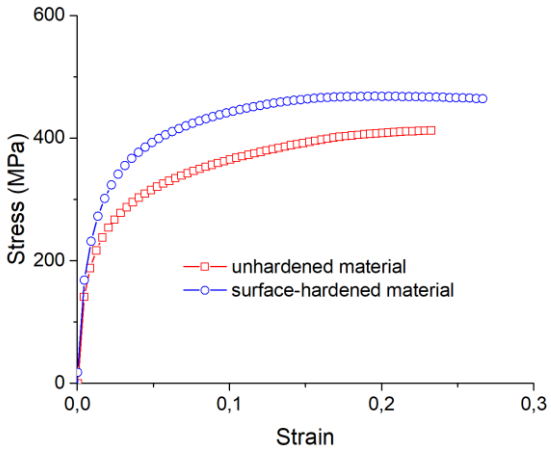

Figure 6. Calculated stress-strain curves for unhardened and UIT surface-hardened polycrystals.

Figure 6 demonstrates the calculated stress-strain curves describing the macroscopic deformation behavior of the model polycrystals under study. The UIT surface-hardened material has better strength characteristics compared to those of the unhardened material. According to the Hall–Petch relation,

the yield stress of the UIT subsurface layer is higher than that of the unhardened material. Correspondingly, the stress-strain curve of the UIT surface-hardened material lies higher. The presence of a basal texture in the subsurface layer additionally increases the strength characteristics. In this case, the in-plane prismatic slip is a primary deformation mode of the subsurface grains while the basal slip is difficult to occur.

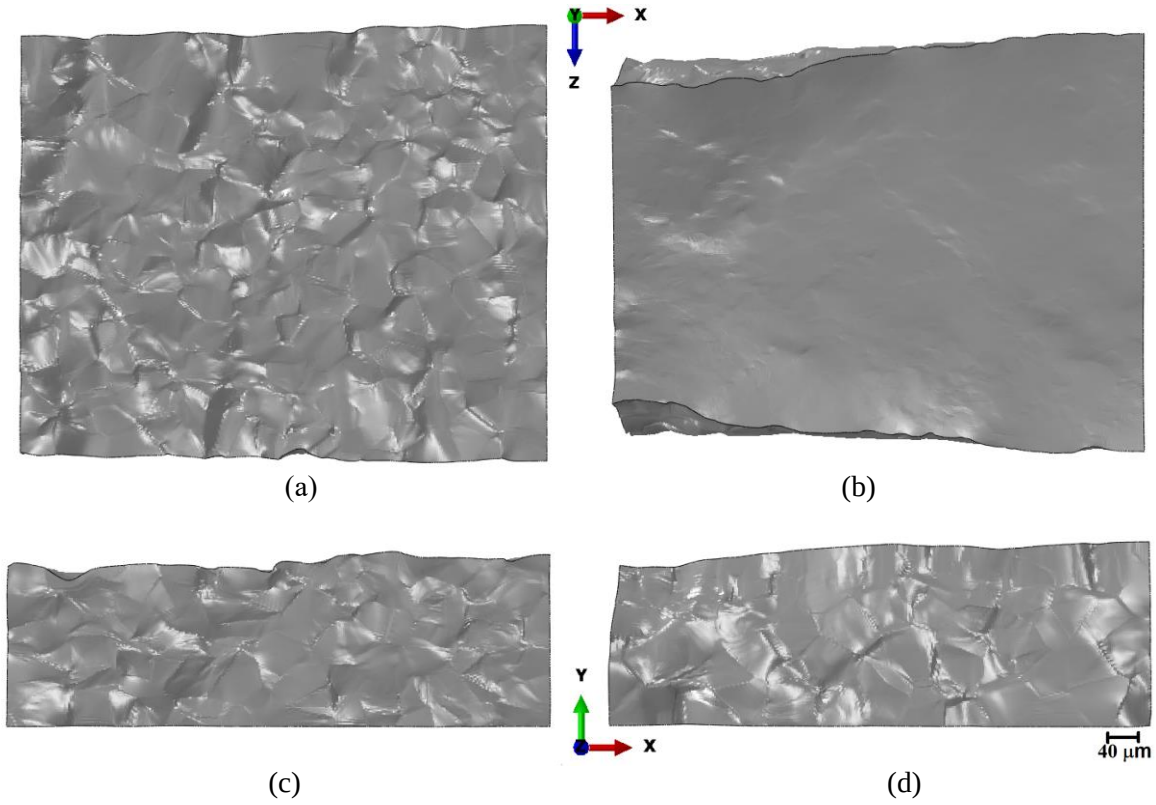

Figure 7. Surface roughness in the unhardened (a, c) and UIT surface-hardened titanium polycrystals (b, d) at 20% tensile strain. Top view (a, b), side view (c, d).

Figure 7 demonstrates the patterns of deformation-induced surface roughness in the XZ- (top view, figure 7 a, b) and XY- (side view, figure 7 c, d) planes in the unhardened (figure 7 a, c) and UIT surface-hardened (figure 7 b, d) model polycrystals at 20% tensile strain. Surface representation is similar to optical microscopy conditions, where a specimen surface is illuminated by a light source located at a certain angle to the surface. The UIT hardened subsurface layer significantly affects the specimen ability to change its shape under uniaxial tension. The basal texture of the subsurface layer leads to suppression of the microscale surface roughness formed by displacements of individual grains perpendicular to the free surface (the orange peel pattern) and mesoscopic surface roughness formed by the displacements of grain groups (figure 7). The basal orientation of grains in the subsurface layer affects the material ability to deform perpendicular to the loading axis, i.e. along the Y- and Z-axes, since the subsurface grains can be deformed only by prismatic slip. The UIT surface-hardened specimen is less strained along the Y-axis and higher strained along the Z-axis than the unhardened polycrystal (cf. figure 6 a, c and b, d).

4. Conclusion

The features of plastic strain localization in polycrystalline titanium surface-hardened by ultrasonic impact treatment have been numerically investigated. Three-dimensional model microstructures inherent in the unhardened (with equiaxed grains without texture) and UIT surface-hardened (with a

basal texture of refined grains in the subsurface layer) titanium specimens were generated by the step-by-step packing method. In order to take into account the deformation mechanisms developing at the micro- and mesoscales, the constitutive equations describing the deformation behavior of individual grains were constructed in the framework of crystal plasticity approach.

A strongly inhomogeneous stress-strain state was shown to develop from the onset of plastic deformation in both specimens. A higher level of stresses was observed in the subsurface layer of the UIT surface-hardened material due to a smaller average grain size. Multiple noncrystallographic shear bands were shown to pass through the grains regardless of their orientations cover the entire specimen surfaces. In the UIT surface-hardened material, the mesoscale shear bands lied at an angle of 45 degrees to the loading axis on the specimen free surface and perpendicular to the loading axis on the lateral sides. Contrastingly, in the unhardened material the mesobands were perpendicular to the loading axis on the free surface and at an angle of 45 degrees on the lateral sides.

The UIT surface-hardened material was shown to have better strength characteristics compared to those of the unhardened material. Both the finer grain size and the presence of a basal texture in the UIT surface-hardened layer were responsible for the increase in the yield strength. The basal texture was found out to suppress the deformation-induced surface roughness at the micro- and mesoscales.

Acknowledgements
This work is supported by the Fundamental Research Program of the State Academies of Sciences for 2013-2020, line of research III.23.

References

[1] Panin A V, Kazachenok M S, Kozelskaya A I, Balokhonov R R, Romanova V A, Perevalova O B and Pochivalov Y I 2017 *Mater Des* **117** 371-81
[2] Panin V E, Panin A V, Perevalova O B, Shugurov A R 2019 *Phys Mesomech* **22(5)** 345-54
[3] Hairullin R, Kozelskaya A and Kazachenok M 2016 *Key Eng Mater* **685** 330–3
[4] Romanova V, Balokhonov R, Panin A, Kazachenok M and Kozelskaya A 2017 *Mater. Sci. Eng.* A **697** 248–58
[5] Panin V E, Panin S V, Pochivalov Yu I, Smirnova A S, Eremin A V 2018 *Phys Mesomech* **21(5)** 464-74
[6] Panin A V, Kazachenok M S, Perevalova O B, Sinyakova E A, Krukovsky K V, Martynov S A 2018 *Phys Mesomech* **21(5)** 441-451
[7] Romanova V A, Balokhonov R R A method of step-by-step packing and its application in generating 3D microstructures of polycrystalline and composite materials 2019 *Engineering with Computers Preprint* 10.1007/s00366-019-00820-2
[8] Diehl M, An D, Shanthraj P, Zaefferer S, Roters F and Raabe D 2017 *Phys Mesomech* **20(3)** 311–23
[9] Harewood F J, McHugh P E 2007 *Comput Mater Sci* **39** 481-94
[10] Hu X, Wagoner R H, Daehn G S, Ghosh S 1994 *Commun Numer Meth En* **10(12)** 993-1003
[11] Kutt L M, Pifko F B, Nardiello J A, Papazian J M 1998 *Comput Struct* **66(1)** 1-17